I&EC research
Industrial & Engineering Chemistry Research
pubs.acs.org/IECR
Article

Accelerating the Development and Transfer of Freeze-Drying Operations for the Manufacturing of Biopharmaceuticals by Model-Based Design of Experiments

Riccardo De-Luca, Gabriele Bano, Emanuele Tomba, Fabrizio Bezzo, and Massimiliano Barolo*

Cite This: *Ind. Eng. Chem. Res.* 2020, 59, 20071−20085
Read Online
ACCESS | Metrics & More | Article Recommendations

ABSTRACT: In the pharmaceutical industry, freeze-drying (also known as lyophilization) is often used to increase the shelf life of heat-sensitive biopharmaceuticals such as protein-based therapeutic drugs and vaccines. The most time- and energy-consuming step of a lyophilization process is primary drying. When a new system configuration (e.g., a new equipment, product formulation, or primary packaging) is to be tested in process development or when transferring to manufacturing facilities, one needs to characterize heat and mass transfer in the new configuration through a battery of experiments that can be very demanding. In this study, we use a model-based design of experiments (MBDoE) to design optimal experiments for fast primary-drying model parameter estimation. We show that MBDoE allows estimating all key heat- and mass-transfer parameters in a statistically meaningful way using one single, optimally designed experiment. Using data from industrial equipment, we test the effectiveness of the methodology on two typical problems to be faced in pharmaceutical process development and transfer: (i) transfer of product manufacturing between two different pieces of equipment and (ii) change of vial type for a given product in a given equipment. Results demonstrate that the proposed methodology can substantially ease the experimentation, thus accelerating the development of freeze-drying operations.

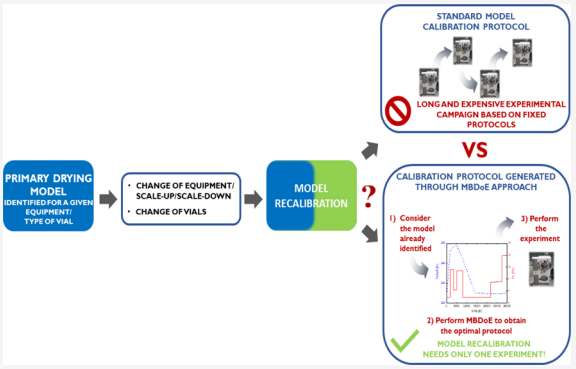

1. INTRODUCTION

Freeze-drying (also known as lyophilization) is used in pharmaceutical manufacturing to stabilize and maintain over time those products that can get degraded in aqueous solutions, such as protein-based therapeutic drugs or vaccines. Freeze-drying is a three-stage process through which a solvent (typically water) is removed from a frozen solution by sublimation.[1,2] The process is typically run batchwise. First, solution-filled semiopen vials are placed over different shelves within a freeze-drying chamber, and their content is frozen (freezing stage). Then, the chamber is evacuated to the desired pressure, and the shelf temperature is increased to get ice sublimation (primary drying stage). During this stage, the heat-transfer fluid (usually silicone oil) circulating within the shelves provides the heat necessary for ice sublimation; the vapor generated by ice sublimation in the chamber is removed through a condenser, which is linked to the chamber through a duct. Finally, the residual water adsorbed onto the resulting solid matrix is completely removed by further heating the shelves at greater temperatures (secondary drying stage). Primary drying is the most energy-intensive step (∼36% of the total exergy input of the process[3]) and is also time-consuming (>50% of the typical total duration of a drying cycle[4]).

Typically, primary drying is carried out at constant values of the shelf temperature and chamber pressure, as determined by experience on running the process in a given equipment, for a given product and vial type. The freeze-dryer is run conservatively to prevent meeting conditions that are critical for the drug structure and that can lead to loss of product quality.[5] For instance, depending on the product formulation, the bulk temperature has to be smaller than the collapse temperature/eutectic temperature of the processed formulation,[6] and the total sublimation flux from the vials must be smaller than the one causing chocked flow to the condenser.[7] The possibility to optimize the operation by adjusting the shelf temperature and chamber pressure has been discussed in some studies.[8−10]

Several freeze-drying models are available in the literature, ranging from simplified one-dimensional models (such as the

Received: June 23, 2020
Revised: October 14, 2020
Accepted: October 16, 2020
Published: November 2, 2020

Downloaded via CARLETON UNIV on November 28, 2020 at 05:18:10 (UTC).
See https://pubs.acs.org/sharingguidelines for options on how to legitimately share published articles.

ACS Publications
© 2020 American Chemical Society

https://dx.doi.org/10.1021/acs.iecr.0c03115
Ind. Eng. Chem. Res. 2020, 59, 20071−20085

ones proposed by Sadikoglu and Liapis[11] and by Velardi and Barresi[12]) to multidimensional models,[13,14] up to more complex computational fluid dynamic models accounting for velocity, pressure, and temperature fields inside the freeze-drying chamber.[15] Although proactively encouraged by the regulatory agencies, the use of freeze-drying first-principles models in industrial pharmaceutical environments (e.g., for design space description, process optimization, process control, continuous process verification[16−18]) is still limited, not only because first-principles models may not be simple to develop but also because the experimental effort required to identify the model parameters can be very significant. The primary drying model parameters are typically related to heat and mass transfer, and their values may be dependent on the equipment in which the process is run, on the specific formulation being manufactured and on the characteristic of the primary packaging (e.g., vial format). Therefore, when a new system configuration (i.e., a new equipment, product, or vial) is used, re-estimation of the relevant model parameters is required, which can be very demanding. Consider, for example, the problem of "product transfer" (PT), that is, transferring the manufacturing of a product across different pieces of equipment (e.g., when scaling-up from R&D to manufacturing or moving the production to different manufacturing sites) or a "change of vials" (CoV) problem, that is, changing (e.g., for type or manufacturer) the main primary packaging of the product. When PT or CoV are to be addressed, a new characterization of the heat- or mass-transfer parameters (or both) is required under the new process configuration, and the experiments required to characterize heat transfer are typically different from those required for mass-transfer characterization. For instance, to characterize the heat-transfer parameters, one would typically need to perform three gravimetric experiments, which are very time-consuming and entail repeatedly weighing a large number of vials.[19] The mass-transfer coefficient is sometimes assumed not to change across different processing units,[20] but this assumption may not be reliable because different units may exhibit different freezing performances[21] and therefore at least one additional lengthy experiment would be required. Clearly, the availability of a systematic protocol for rapid characterization of heat and mass transfer across different units, packaging, or formulations would significantly contribute to accelerate the development of pharmaceutical freeze-drying operations.

In this study, we propose model-based design of experiments (MBDoEs[22]) to design highly informative dynamic experiments that enable reducing the number and complexity of experimental tests required to characterize the heat- and mass-transfer phenomena in a freeze-dryer whenever a new system configuration is to be considered. MBDoE has been widely exploited in several application domains[23−26] including the pharmaceutical one, proving itself as a cross-cutting tool to avoid unnecessary iterations in process development cycles and to speed up process validation tasks.[27,28] Here, we prove the effectiveness of MBDoE to accelerate the development of freeze-drying operations when a model validated for a given source configuration (base case) is available, and the task is to rapidly reidentify the key model parameters under PT or CoV configuration changes (target configurations). Namely, we show that one single, optimally designed experiment can be sufficient to obtain statistically meaningful estimates of all the key model parameters related to heat and mass transfer.

The article is structured as follows. In Section 2, we first describe the experimental setup and present the basic idea we propose; then, we provide a detailed discussion of the primary drying model; finally, after describing the rationale of conventional MBDoE, we focus on its application to the freeze-drying case. In Section 3, we present and discuss the results obtained for the two configuration changes described above. In Section 4, we summarize the results obtained, and we propose some suggestions for future work.

2. PROCESS AND MODEL

In this section, we first present the experimental setup and discuss the rationale behind the proposed MBDoE approach for fast model identification; then, we describe the primary drying model; afterward, we introduce some mathematical background on MBDoE and discuss its formulation for the current study; finally, we provide some details on the software used to carry out all model-based activities.

2.1. Experimental Setup. The base case is characterized by the following configuration: (i) a partially loaded (one tray out of a total of five, corresponding to 476 vials) VirTis Genesis 25EL freeze-dryer (EQUIP #1, SP Scientific, Stone Ridge, NY, USA; see Figure 1a) and (ii) 3 mL nonsiliconized vials (Müller & Müller, Holzminden, Germany; VIAL #1) filled with 0.6 mL of 5% w/w sucrose solution.

(a) (b)

Figure 1. Photograph of a front view of (a) EQUIP #1 (VirTis Genesis 25EL freeze-dryer); (b) EQUIP #2 (Lyostar 3 freeze-dryer).

The two target configurations are defined as follows.

2.1.1. Product Transfer. We process the same formulation inside the same type of vials as in the base case but using a different freeze-dryer. The task is estimating the model parameters when changing the freeze-drying unit from EQUIP #1 to a Lyostar 3 freeze-dryer (SP Scientific, Stone Ridge, NY, USA; EQUIP #2; see Figure 1b) using VIAL #1. Similar to the base case, we considered partial loading (one tray out of a total of four, corresponding to 560 vials) also in EQUIP #2. From an industrial perspective, this case study is representative of PT/scale-up between different facilities, when the lyophilization recipe may need readjustment as a consequence of the characteristics of the equipment the manufacturing is transferred to.

2.1.2. Change of Vials. We process the same formulation in the same freeze-dryer as in the base case but using a different type of vials. The task is estimating the model parameters when using 3 mL siliconized vials (Gerresheimer AG, Dusseldorf,

https://dx.doi.org/10.1021/acs.iecr.0c03115
Ind. Eng. Chem. Res. 2020, 59, 20071−20085

Germany; VIAL #2) instead of nonsiliconized ones (VIAL #1) in EQUIP #1. From an industrial perspective, this case study represents situations where process development requires changes (such as testing of different primary packaging, implementation of different formats, introduction of vials from different suppliers in manufacturing) whose impact on the attribute of a given product has to be verified.

The equipment and vial types used in the study (and their acronyms) are summarized in Table 1.

Table 1. Equipment and Vials Used in This Study

category	description	manufacturer	acronym
equipment	VirTis Genesis 25EL	SP Scientific, Stone Ridge, NY, USA	EQUIP #1
	Lyostar 3	SP Scientific, Stone Ridge, NY, USA	EQUIP #2
vial	nonsiliconized vial	Müller &; Müller, Holzminden, Germany	VIAL #1
	siliconized vial	Gerresheimer AG, Dusseldorf, Germany	VIAL #2

We assume that a mathematical model describing the primary drying phase is available and that its reliability to describe the base case has been preliminarily assessed by a validation experiment. For any of the two target configurations described above, we propose the following three-step procedure to accelerate PT or CoV (Figure 2):

Step 1. Use MBDoE to design one maximally informative experiment to identify all model parameters in the target configuration.

Step 2. Perform the experiment designed in step 1 in the target configuration and estimate the model parameters in that configuration using the resulting experimental data.

Step 3. Given the new estimates on model parameters, validate the model for the target configuration with (at least) one further experiment (no need to design it through MBDoE).

Note that if statistical significance for all model parameters is not achieved in step 2, one would need to iterate the procedure by designing a new experiment (step 1) using the parameter estimates obtained in step 2 and then proceeding with the other steps.[29] For the model calibration and validation steps, we used the following equipment measurements: (i) frozen-layer bulk temperature readings (T_B [K]) provided by T-type, copper-constantan wire, AWG 24 thermocouples placed inside vials selected according to their topological distribution on the tray; and (ii) drying chamber pressure as recorded from both a Pirani gauge (P^{Pir} [Pa]) and a capacitive manometer (P^{CM} [Pa]). With reference to thermocouple placement inside the vials, we took care to avoid incorrect positioning as discussed by Demichela et al.[30] Furthermore, the combined exploitation of temperature and pressure measurements for the parameter estimation task helped reducing potential errors related to thermocouple effects on product structure.[10]

Figure 3a,b shows a subset of the time profiles recorded by the available measurement system from a typical freeze-dryer run. The bulk temperature readings in Figure 3a come from five different thermocouples (indicated as TI1, TI3, TI5, TI6, and TI7). Note that each temperature profile shows an inflection point (marked with a cross in the figure) right before a rise in temperature. The inflection point (whose time location depends on the location of the vial on the shelf and on the positioning of the thermocouple in the vial) indicates the instant at which the sublimation front crosses the tip of the thermocouple.

This means that, from that time on, the registered temperature measurement can no longer be referred to the frozen product and consequently cannot be used to calibrate, validate, or exploit the primary drying model (presented in the next section). As will be discussed in Section 2.2.3 and as shown in Figure 3c, in this study we adopted a logical partition of the freeze-dryer shelf into two different zones (inner and outer). For model calibration, we used the lowest recorded temperature profile in the inner zone of the shelf and the highest recorded temperature profile in the outer zone. We chose to use these two sensor readings so as to capture the slow sublimation dynamics of the vials in the inner zone and to handle the constraint on the product collapse temperature conservatively, that is, by assuming that all the vials allocated in the outer zone follow the highest measured product temperature profile.

The (somewhat noisy) pressure profiles shown in Figure 3b highlight the typical behavior of the Pirani measurement with respect to the one of the capacitance sensor reading. The instant at which P^{Pir} starts to rapidly decline (onset) indicates that the vapor phase in the chamber is starting to change from mostly water to mostly nitrogen, whereas the instant at which P^{Pir} flattens (offset) indicates the practical end of the primary drying phase, when almost exclusively nitrogen is present in the drying chamber.[31] The midpoint in between indicates a change of concavity of the Pirani pressure curve. Note that the signal $y_{meas} = P^{Pir} - P^{CM}$ is used to calibrate, validate, or exploit the primary drying model (to be described in the next section).

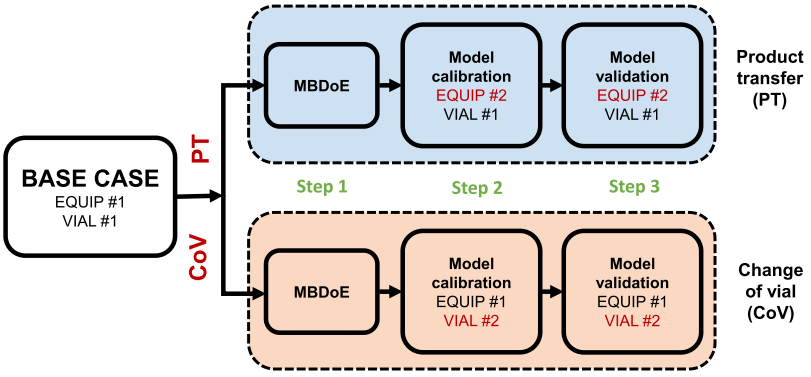

Figure 2. Schematic view of the methodology proposed in this study to accelerate the development of freeze-drying operations using MBDoEs.

https://dx.doi.org/10.1021/acs.iecr.0c03115
Ind. Eng. Chem. Res. 2020, 59, 20071−20085

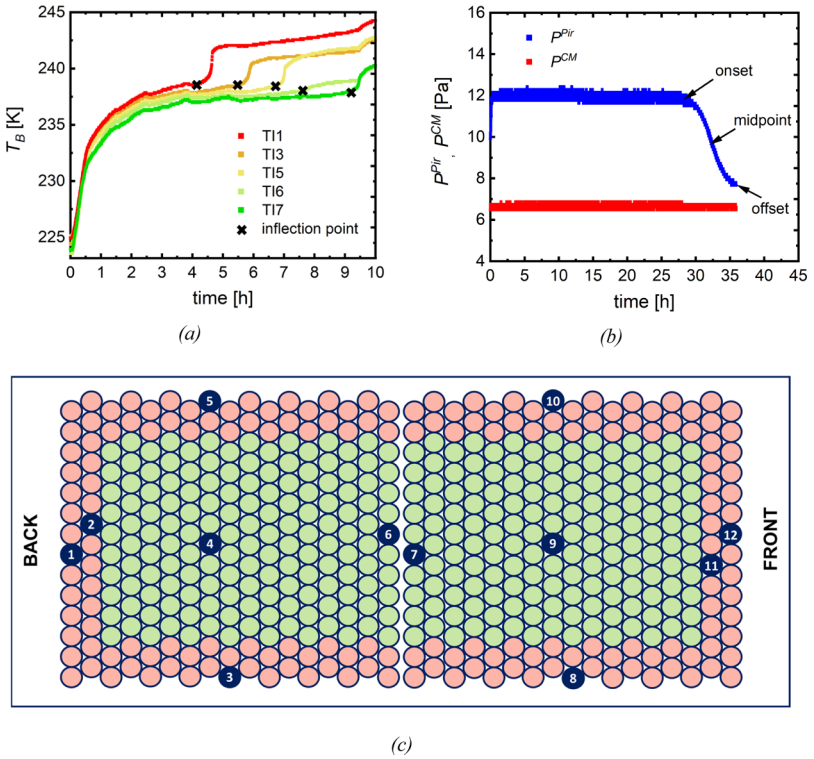

Figure 3. EQUIP #1: an example of some measurements recorded during a typical freeze-drying run and illustration of the partitioning of the shelf into an inner zone and an outer zone. (a) Bulk temperature profiles as measured by a subset of the available thermocouples (the black crosses indicate the inflection points). (b) Pressure profiles as measured by the Pirani gauge and the capacitive manometer (with indication of onset, midpoint, and offset times). (c) Logical partitioning of the shelf into an inner zone (green) and an outer zone (red), with indication of the locations of the available set of thermocouples (black circles).

Trelea et al.[32] suggested to infer the water partial pressure $P_{w,c}^{exp}$ [Pa] in the chamber from pressure readings according to

$$\frac{y_{meas}}{0.6} = P_{w,c}^{exp} \tag{1}$$

To account for potential differences in the Pirani pressure sensor calibration when different pieces of equipment are used and to account for possible sensor adjustment during equipment maintenance, in this study, we propose a more general formulation

$$\frac{y_{meas}}{0.6} = P_{w,c}^{exp} + P_{bias} - \gamma(P^{CM} - P_{cal}) \tag{2}$$

where P_{cal} [Pa] is the pressure at which the Pirani gauge is calibrated (4 Pa, in this study) and P_{bias} [Pa] and γ [-] are corrective parameters whose values are to be determined. We attenuated noise in the pressure measurements by filtering both P^{Pir} and P^{CM} with a low pass filter.

2.2. Primary Drying Mechanistic Model. In this study, we described primary drying through the model proposed by Fissore et al.,[16] with the following improvements: (i) a dynamic energy balance to describe the time-varying thermal inertia of the system; (ii) the water partial pressure dynamics as dependent on the balance between the total sublimation mass flow and the condensed vapor mass flow.[14] The purpose of using the model is to describe the behavior of the vials inside the freeze-drying chamber in such a way as to reliably predict key performance indicators of the process, such as the sublimation end time and the maximum temperature reached by the product. The key model equations are described in the following.

2.2.1. Energy Balance. We assumed that radial temperature gradients within the product are negligible[13] and that each vial contains the same amount of ice at the beginning of a drying cycle. The frozen-layer bulk temperature T_B is calculated through the following energy balance

$$\rho_f c_{p,f} A_{b,v} \frac{d(L_f T_B)}{dt} = Q_{w,v} + Q_{r,v} + Q_{s,v} - \Delta H_{sub} J_w A_{b,v} \tag{3}$$

where ρ_f is the frozen layer density [kg m^{-3}], $c_{p,f}$ [J kg^{-1} K^{-1}] is the specific heat capacity of the frozen layer, $A_{b,v}$ [m^2] is the vial bottom area, L_f [m] is the length of the frozen layer inside the vial, ΔH_{sub} [J kg^{-1}] is the heat of sublimation, and J_w is the mass sublimation flux [kg m^{-2} s^{-1}]. The three terms $Q_{w,v}$, $Q_{r,v}$, and $Q_{s,v}$ [J s^{-1}], respectively, represent the rates of heat transfer from the chamber walls to the vials, from the rails in which vials are framed (if applicable) to the vial surface, and from the shelf to the vial bottom. These rate terms are calculated from[10,14]

$$Q_{w,v} = a_1 \sigma_{SB}(\overline{T}_W^{\,4} - T_B^{\,4}) \tag{4}$$

$$Q_{r,v} = a_2 \sigma_{SB}(\overline{T}_r^{\,4} - T_B^{\,4}) \tag{5}$$

$$Q_{s,v} = (K_{cond} + K_{rad}) A_{b,v}(T_{shelf} - T_B) \tag{6}$$

where $\overline{T}_W$ [K] is the mean temperature of the chamber walls, $\overline{T}_r$ [K] is the mean temperature of the rails, T_{shelf} [K] is the shelf temperature, and σ_{SB} [W m^{-2} K^{-4}] is the Stefan–Boltzmann constant.

https://dx.doi.org/10.1021/acs.iecr.0c03115
Ind. Eng. Chem. Res. 2020, 59, 20071−20085

Both $Q_{w,v}$ and $Q_{r,v}$ in eqs 4 and 5 are pure radiant contributions described through modified Stefan−Boltzmann laws; a_1 [m^2] and a_2 [m^2] are equipment-dependent parameters to be estimated. K_{cond} and K_{rad} [W m^{-2} K^{-1}] in eq 6 describe the shelf-vial heat transfer because of conduction (through both the vial glass and the gas entrapped between the bottom of the vials and the shelf) and radiation, respectively, according to[12,20]

$$K_{cond} = C_1 + \frac{C_2 P_c}{1 + C_3 P_c} \tag{7}$$

$$K_{rad} = a_3 \sigma_{SB} (T_{shelf} + T_B)({T_{shelf}}^2 + {T_B}^2) \tag{8}$$

where a_3 [-], C_1 [W m^{-2} K^{-1}], C_2 [W m^{-2} K^{-1} Pa^{-1}], and C_3 [Pa^{-1}] are parameters to be estimated, whereas P_c is the chamber pressure [Pa]. Note that, following Pikal et al.,[33] the contribution to heat transfer because of convection is neglected.

2.2.2. Mass Balance. The mass balance of the solid phase inside the vial is modeled as

$$\frac{dL_f}{dt} = -\frac{1}{\rho_f - \rho_d} J_w \tag{9}$$

where ρ_d is the dried layer density [kg m^{-3}] and J_w is expressed as

$$J_w = \frac{1}{R_p}(P_{w,int} - P_{w,c}) \tag{10}$$

The term $P_{w,int}$ [Pa] is the partial pressure of water at the sublimation interface, $P_{w,c}$ [Pa] is the partial pressure of water in the chamber, and R_p [m s^{-1}] is the resistance to mass transfer, calculated through the following expression[34]

$$R_p = R_0 + \frac{A(L_0 - L_f)}{1 + B(L_0 - L_f)} \tag{11}$$

where R_0 [m s^{-1}] is the formulated product mass-transfer resistance at the beginning of the primary drying phase, A [s^{-1}] and B [m^{-1}] are fitting parameters, and L_0 [m] is the initial height of the frozen layer. The term $P_{w,int}$ [Pa] is calculated using a modified version of the Goff−Gratch correlation as proposed by Fissore et al.[35]

$$P_{w,int} = \exp\left(-\frac{6139.9}{T_B[K]} + 28.8912\right) \tag{12}$$

Although $P_{w,int}$ is related to the solid−vapor interface temperature in the original correlation, in this study we used the vial bulk temperature T_B, assuming negligible axial temperature gradient in the vial for the case studies under investigation. This assumption holds true for pharmaceutical formulations processed in vials loaded with a relatively small product volume within freeze-drying units because the heat transfer along the frozen material is faster than the heat transfer between the shelves and the vial bottom.[36,37]

2.2.3. Dynamics of the Water Partial Pressure. The water partial pressure $P_{w,c}$ is described according to the following equation[14]

$$\frac{dP_{w,c}}{dt} = \frac{R_g \bar{T}_W}{V_c M_w}(\dot{m}_s^{tot} - \dot{m}_{cd}) \tag{13}$$

where R_g [J mol^{-1} K^{-1}] is the ideal gas constant, V_c [m^3] is the volume of the drying chamber, and M_w [kg $kmol^{-1}$] is the molar mass of water. The water vapor flow to the condenser ($\dot{m}_{cd}$ [kg s^{-1}]) is calculated following Trelea et al.[32]

$$\dot{m}_{cd} = \frac{1}{\alpha_{cd}\bar{T}_{cd}} \log\left(\frac{P_c - P_{w,cd}}{P_c - P_{w,c}}\right) \tag{14}$$

where $\bar{T}_{cd}$ [K] is the mean temperature of the condenser, α_{cd} [s kg^{-1} K^{-1}] is an equipment-dependent parameter to be estimated, and $P_{w,cd}$ is the water vapor pressure at the condenser surface, calculated by replacing T_B with $\bar{T}_{cd}$ in eq 12. The term $\dot{m}_s^{tot}$ [kg s^{-1}] in eq 13 is the total sublimation mass flow, computed as the sum of the contributions of each vial inside the drying chamber. Mathematically, we described it as follows

$$\dot{m}_s^{tot} = \sum_{i=1}^{N_V} A_{b,v} J_{w,i} \qquad i = 1, ..., N_v \tag{15}$$

where N_V is the number of vials and $J_{w,i}$ is the sublimation flow rate of the ith vial inside the chamber. Note that eq 15 links the behavior of the single vial to the behavior of the whole vial bed, thus determining the macroscopic process performance. Different approaches can be considered to describe vial-to-vial variability.

2.2.4. Total Homogeneity. All vials inside the freeze-dryer have the same behavior, and the total sublimation flow is given by the product of the sublimation flow from a single vial and the total number of vials (i.e., $\forall i \in [1, N_V]$ $J_{w,i} = J_w$). This modeling approach is useful if the final aim is the following:

a) either obtaining a safe protocol only for the majority of the vials inside the chamber (all vials = inner vials), while not guaranteeing that the required quality is met for the product contained in the outer vials. In fact, because of the expected greater radiation contribution caused by the proximity of the outer vials to the chamber wall, the temperature of the outer vials may become greater than the product collapse temperature;
b) or obtaining a conservative protocol (all vials = outer vials) to ensure consistent product quality for all vials, at the expense of the total duration of the process. In this case, the assumption that all vials behave as the outer ones would lead to longer operation because central vials are characterized by smaller sublimation rates and lower temperatures than outer vials.

2.2.5. Total Heterogeneity. N_V different values of $J_{w,i}$ must be calculated to consider vial-dependent physical mechanisms because of local temperature and pressure gradients.[10,14] Consequently, the mass- and heat transfer-dependent parameters reported in eqs 3−12 must be identified for each vial, hence dramatically increasing both the model complexity and the computational cost related model identification.

2.2.6. Multizone Homogeneity. A number of zones are defined (according to a "topologic" rationale) in the shelf, and each vial is allocated to one zone; all the vials allocated to the same zone are assumed to behave in the same way.[21] Mathematically, this assumption leads to the following modification to eq 15:

$$\dot{m}_s^{tot} = \sum_{i=1}^{N_{zones}} N_V f_{v,i} A_{b,v} J_{w,i} \qquad i = 1, ..., N_{zones} \tag{16}$$

https://dx.doi.org/10.1021/acs.iecr.0c03115
Ind. Eng. Chem. Res. 2020, 59, 20071−20085

Table 2. List of Fixed Model Parameters[a]

parameter	symbol	value	units	reference
Physical Constants				
ideal gas law constant	R_g	8.3145	J mol^{-1} K^{-1}	
Stefan−Boltzmann constant	σ_{SB}	5.6704×10^{-8}	W m^{-2} K^{-4}	
molecular weight of water	M_w	18.01	kg kmol^{-1}	
Frozen Product (Ice) Physical Properties				
density	ρ_f	917	kg m^{-3}	37
heat of sublimation	ΔH_s	2.8×10^6	J kg^{-1}	37
specific heat capacity	$c_{p,f}$	2108	J kg^{-1} K^{-1}	
Formulation-Dependent Physical Properties				
density of the dried product (sucrose 5% w/w)	ρ_d	63	kg m^{-3}	18
initial mass transfer resistance (sucrose 5% w/w)	R_0	5.12×10^4	m s^{-1}	36
Equipment-Dependent Parameters				
EQUIP #1 chamber volume	$V_C^{\#1}$	0.118	m^3	
EQUIP #2 chamber volume	$V_C^{\#2}$	0.316	m^3	
EQUIP #1 total number of vials	$N_V^{\#1}$	476		
EQUIP #2 total number of vials	$N_V^{\#2}$	560		
EQUIP #1 Fraction of inner vials	$f_{V,1}^{\#1}$	0.78		
EQUIP #2 Fraction of inner vials	$f_{V,1}^{\#2}$	0.68		
Other Fixed Parameters				
vial diameter	d_v	0.01455	m	
mean rail temperature	$\bar{T}_r$	250.15[a]	K	
mean wall temperature	$\bar{T}_w$	276.15[a]	K	

[a]Average value estimated by placing thermocouples at different wall/rail locations inside the chamber of the VirTis Genesis 25EL freeze-dryer (EQUIP #1).

subject to

$$\sum_{i=1}^{N_{zones}} f_{v,i} = 1 \tag{17}$$

where N_{zones} is the number of zones and $f_{v,i}$ is the fraction of total vials allocated to the ith zone.

As anticipated in Section 2.1 (Figure 3c), in this study we adopted the latter approach by logically partitioning the shelf into two different zones (inner and outer, the latter corresponding to the two outermost rows of vials along the shelf perimeter). This choice is a tradeoff between two competing requirements: (i) differentiating between vials located in different positions inside the drying chamber (as discussed earlier, outer vials that are directly exposed to the chamber walls are affected by greater radiation, whereas inner vials are less affected by radiation because of the shielding effect of the external vials) and (ii) limiting the number of model parameters to be estimated. Although the two-zone description may appear oversimplified, it nevertheless allows calculating the key performance indicators with good accuracy for practical use.

A list of physical constants and fixed-value parameters used in this study is reported in Table 2. The model parameters to be identified are listed in Table 3; further details on a simplification of the parameter set will be discussed in Section 3.

2.3. Model-Based Design of Experiments. The target of conventional MBDoE is the reduction of the model parameter uncertainty region through the optimization of the experiment design vector $\boldsymbol{\varphi}$, expressed in its more general form as

$$\boldsymbol{\varphi} = [\mathbf{y}_0,\ \mathbf{u}(t),\ \mathbf{w},\ \mathbf{t}^{sp},\ \tau]^T \tag{18}$$

where $\mathbf{y}_0$ is the set of initial conditions for the measured variables; $\mathbf{u}(t)$ and $\mathbf{w}$ are the time-dependent and time-invariant manipulated inputs, respectively; $\mathbf{t}^{sp}$ is the vector of the output variables sampling times; and τ is the total duration of the experiment. The mathematical formulation of the optimization problem can be described as follows

Table 3. List of the Overall Set of Model Parameters to be Identified

	Parameter	
inner zone	mass transfer	R_0, A, B
	heat transfer	a_1, a_2, a_3, C_1, C_2, C_3
outer zone	mass transfer	R_0, A, B
	heat transfer	a_1, a_2, a_3, C_1, C_2, C_3
condenser	α_{cd}	
corrective parameters	P_{bias}, γ	

$$\boldsymbol{\varphi}^{opt} = \arg\min_{\boldsymbol{\varphi}} \{\psi[\mathbf{V}_\theta(\boldsymbol{\theta},\ \boldsymbol{\varphi})]\} \tag{19}$$

subject to

$$f(\dot{\mathbf{x}}(t),\ \mathbf{x}(t),\ \mathbf{u}(t),\ \mathbf{w},\ \boldsymbol{\theta},\ t) = 0 \tag{20}$$

$$\hat{\mathbf{y}} = h(\mathbf{x}) \tag{21}$$

$$\mathbf{x}(t) - \mathbf{G}(t) \le 0 \tag{22}$$

$$\varphi_i^l \le \varphi_i \le \varphi_i^u, \qquad i = 1, \ldots, n_\varphi \tag{23}$$

where $\boldsymbol{\varphi}^{opt}$ is the optimal design vector. The term $\mathbf{V}_\theta$ in eq 19 is the expected variance-covariance matrix of the model parameter set $\boldsymbol{\theta}$, whereas ψ is a metric of $\mathbf{V}_\theta$ and represents the criterion chosen for the experiment design. Typically, this metric is set to equal to the determinant (D-optimal criterion), the trace (A-optimal criterion) or the maximum eigenvalue (E-optimal criterion) of $\mathbf{V}_\theta$.[38,39] Function $f(\cdot)$ in eq 20 is a differential-algebraic system implicit function, and $h(\cdot)$ in eq 21 is the function that selects the estimated responses $\hat{\mathbf{y}}$ within the

https://dx.doi.org/10.1021/acs.iecr.0c03115
Ind. Eng. Chem. Res. 2020, 59, 20071−20085

set of model state variables $\mathbf{x}$. $\mathbf{G}(t)$ in eq 22 represents the set of active time-dependent constraints on state variables, whereas eq 23 represents the set of constraints on each element of the design vector $\boldsymbol{\varphi}$, expressed by lower (superscript l) and upper (superscript u) bounds.In this study, we evaluated $\mathbf{V}_\theta(\boldsymbol{\theta}, \boldsymbol{\varphi})$ as[40]

$$\mathbf{V}_\theta(\boldsymbol{\theta}, \boldsymbol{\varphi}) = \left[(\mathbf{V}_\theta^0)^{-1} + \sum_{k=1}^{N_{sp}} \sum_{i=1}^{N_y} \sum_{j=1}^{N_y} s_{ij} \left[\frac{\partial \hat{y}_i(t_k)}{\partial \theta_l} \frac{\partial \hat{y}_j(t_k)}{\partial \theta_m} \right]_{l,m=1,..,N_\theta} \right]^{-1} \tag{24}$$

where s_{ij} is the ijth element of the inverse of the measurement error covariance matrix, N_θ is the number of model parameters, N_y is the number of measured variables, and N_{sp} is the number of samples. From a practical point of view, the two terms within the square brackets of the right-hand side of eq 24 represent (respectively) the inverse of the preliminary parameter variance/covariance matrix $\mathbf{V}_\theta^0$ (i.e., initial uncertainty on parameter values) and the information gain obtained by collecting all the samples for each measured variable during the experiment to be designed.

Conventional MBDoE is typically a three-step procedure that consists of (i) choosing a design criterion and designing the optimal experiment through the optimization of $\boldsymbol{\varphi}$; (ii) executing the designed experiment by implementing the vector $\boldsymbol{\varphi}^{opt}$ obtained in the previous step; and (iii) estimating the parameter set at the end of the experiment. Note that, in principle, these three activities can be repeated sequentially in case statistically unsatisfactory estimates are obtained after the first attempt.[29]

One of the most widely used statistics for assessing the precision in parameter estimation is the t-value ($t_{\theta_i}^{1-\alpha}$) at $(1-\alpha)$% confidence level for the relevant parameters because of its direct link to the information gained during the experimental run. This statistic can be expressed as

$$t_{\theta_i}^{1-\alpha} = \frac{\theta_i}{t(1-\alpha/2,\ N_{sp}-N_\theta)\sqrt{v_{ii}}} \tag{25}$$

where θ_i is the ith component of $\boldsymbol{\theta}$; $t(\cdot)$ at the denominator is the critical value of a t-distribution with $(1-\alpha/2)$% confidence level and $(N_{sp}-N_\theta)$ degrees of freedom, and v_{ii} is the iith term of the parametric variance-covariance matrix. A statistically satisfactory parameter estimation is reached for all the model parameters if each parametric t-value calculated using eq 25 is greater than the reference t-value ($t_{ref}^{1-\alpha}$) at $(1-\alpha)$% confidence level, that is, the critical value of a t-distribution with $(1-\alpha)$% confidence level and $(N_{sp}-N_\theta)$ degrees of freedom, defined as

$$t_{ref}^{1-\alpha} = t(1-\alpha,\ N_{sp}-N_\theta) \tag{26}$$

We set the significance level α% equal to 5% (i.e., we set the confidence level equal to 95%).

2.3.1. MBDoE Applied to the Primary Drying Model. In all simulations discussed in this study, we initialized the primary drying model as follows. The initial freezing phase (occurring before the onset of primary drying) is carried out at the set point rate of −1 K/min down to 223.15 K, and the shelf temperature T_{shelf} is set equal to 223.15 K at the beginning of primary drying. The initial value of the bulk temperature is equal to the value reached by T_{shelf} at the end of the freezing phase. Note that T_{shelf} is not directly accessible to measurement for all vials positions. For the purpose of this study, we set T_{shelf} equal to the measured silicone oil temperature at the shelf entrance. No significant difference between this temperature measurement and the set-point of the shelf temperature controller was found in any of the experiments. The initial length of the frozen layer L_f is equal to 3.609 mm. The initial value of y_{meas} is equal to the value for which, according to eq 2, the partial pressure of water in the chamber is 70% of the chamber pressure P_c, assuming that P_{bias} [Pa] and γ [-] are equal to zero (this assumption derives from observations at the beginning of primary drying of historical experiments). Note that Gaussian noise with zero mean and a standard deviation of 0.2 K and 0.1 Pa is added to the simulated values of T_B and y_{meas}, respectively. The standard deviation values derive from analysis of historical data for the available sensors.

For the optimal design of a freeze-drying experiment, the general formulation of the MBDoE problem can be simplified by considering that the optimal control vector $\boldsymbol{\varphi}$ is only made by the time-profiles of the manipulated inputs, namely, T_{shelf} (typical operating range [223.15, 255.15] K) and P_c (typical operating range [5, 15] Pa), that is,

$$\boldsymbol{\varphi} = \mathbf{u}(t)^T \tag{27}$$

We discretized the input profiles using a control vector parameterization technique.[41] Namely, we set the time profiles of T_{shelf} and P_c as piecewise linear and piecewise constant (respectively), over 10 switching intervals each (note that the process control interface in EQUIP #1 allows setting up to 14 switching intervals for each input). We set the measurement interval equal to 30 s, and the total duration τ of a designed experiment equal to 10 h; this value is a rough estimate, based on historical experimental data, of the average time at which the bulk temperature profiles registered for the inner zone inflect. Note that a designed experiment can in principle be run also beyond that time at given values of T_{shelf} and P_c, but for $t > \tau$, it will not be possible to use the model to represent the actual bulk temperature profile.

To optimally design the experiments, we used the determinant of the parameter variance-covariance matrix (D-optimal criterion) as the experiment information metric. Unlike other commonly used experimental procedures, one significant advantage of MBDoE is the possibility to include process and product constraints at the experiment design level. As for the inequality constraints to be fulfilled (eq 22), we implemented the following ones: (i) the outer zone temperature must not exceed 240.15 K (glass transition temperature for the investigated formulation) and (ii) the total sublimation flow must be smaller than 1.83×10^{-5} kg s^{-1} to avoid chocked flow to the condenser (this value corresponds to the maximum sublimation flow that can be processed in EQUIP #1 in experiments with vials filled with water on a fully loaded equipment[10]). For the parameter estimation exercise after the execution of the designed experiment, we also enforced the length of the frozen layer for the inner zone to be equal to zero at the offset. Although this latter constraint is conservative (as it implies that all the inner vials end sublimation at the offset, thus neglecting the actual heterogeneity of the inner zone), it nevertheless allows the model to improve the prediction of the sublimation phase end-point.

2.4. Software. We used gPROMS Model Builder v.5.1 for process simulation, experiment design, and parameter

https://dx.doi.org/10.1021/acs.iecr.0c03115
Ind. Eng. Chem. Res. 2020, 59, 20071−20085

Table 4. Parameter Values for the Base Case

zone	parameter [units]	estimate	std. deviation	*t*-value 95%
inner zone	A [s^{-1}]	2.13×10^{8}	2.42×10^{5}	449.8
	a_1 [m^2]	4.66×10^{-5}	2.08×10^{-7}	114.1
	C_2 [W m^{-2} K^{-1} Pa^{-1}]	0.27	1.89×10^{-3}	71.3
outer zone	A [s^{-1}]	3.90×10^{8}	7.05×10^{6}	28.2
	a_1 [m^2]	1.06×10^{-4}	4.49×10^{-6}	119.9
	C_2 [W m^{-2} K^{-1} Pa^{-1}]	0.28	1.08×10^{-2}	13.6
condenser	α_{cd} [s kg^{-1} K^{-1}]	2.13×10^{8}	2.42×10^{5}	176.1
		reference *t*-value 95%		1.645

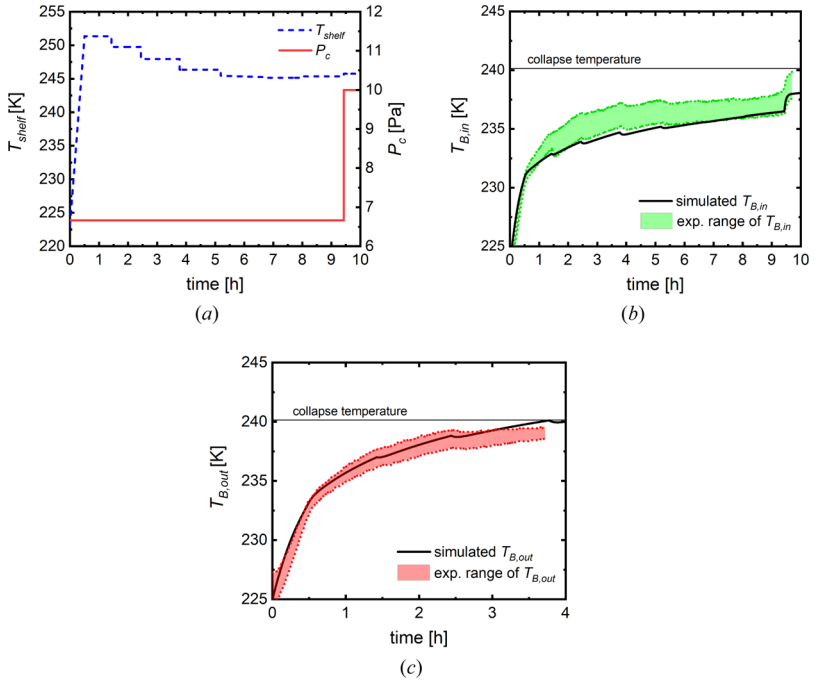

Figure 4. Base case: model validation. Time profiles of (a) actual shelf temperature and chamber pressure; (b) bulk temperature in the inner zone as simulated by the model and as measured in the equipment; (c) bulk temperature in the outer zone as simulated by the model and as measured in the equipment. The experimental temperature profiles in a zone are reported as the range between the maximum and minimum readings from the sensors in that zone.

estimation. Solution of the model was obtained using the DAEBDF solver, design of the experiments was obtained with the default NLPSQP solver, parameter estimation was performed using a maximum likelihood estimator. We performed all activities on an Intel Core I7-9750H CPU@ 2.60 GHz processor with 16.0 GB RAM.

3. RESULTS AND DISCUSSION

In this section, we first present the parameter estimates and the two-zone model performance in the validation experiment performed for the base case configuration. Then, we discuss the optimal experiments designed for the two new configurations (PT and CoV). Finally, for each new configuration, we discuss the model identification results in terms of parameter estimate precision and model goodness-of-fit and evaluate the model prediction performance through a validation experiment.

3.1. Base Case. As discussed in Section 2.1, the base case refers to the reference configuration characterized by EQUIP #1 and VIAL #1. The model involves three parameter sets: mass transfer-related parameters (R_0; A; B), heat transfer-related parameters (C_1; C_2; C_3; a_1; a_2; a_3), and a condenser-related parameter (α_{cd}).

With respect to the mass-transfer parameters, we assigned R_0 the value reported in Table 2, assuming it depends on the investigated formulation (sucrose solution). Following the two-zone modeling assumption, we estimated two different values for A (one for the inner zone and one for the outer zone) because the quality of the frozen product may vary with the vial position inside the chamber.

As for the heat-transfer parameters, we set $C_1 = 2.825$ W m^{-2} K^{-1} as suggested by Bano et al.,[10] and we estimated two different values for C_2 to account for the slight dependence of this parameter on the actual temperature of the gas entrapped between the shelf and the vial bottom,[19] which may vary between the inner and the outer zones. Moreover, we estimated two sets of values both for a_1 and for a_3 to account for the zone-dependent impact of radiation.

Preliminary sensitivity studies showed that the sensitivity of the bulk temperature to parameters B, a_2 and C_3 is limited (in agreement with the experimental findings of Bano et al.[10] and Scutellà et al.[37]). For this reason, we decided not to include them into the set to be estimated and to use historical values of

https://dx.doi.org/10.1021/acs.iecr.0c03115
Ind. Eng. Chem. Res. 2020, 59, 20071−20085

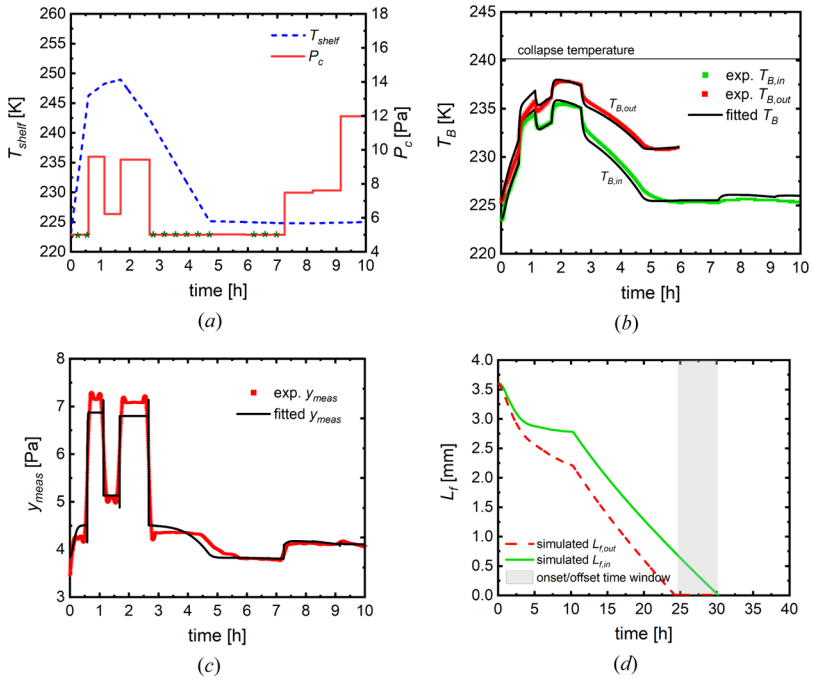

Figure 5. PT: model calibration using an optimally designed experiment. Time profiles of (a) actual shelf temperature and chamber pressure as dictated by the optimally designed experiment (the green stars indicate pressure or temperature values that hit lower/upper bounds); (b) bulk temperature in the inner and outer zones as simulated by the model and as measured in the equipment; (c) difference between the Pirani and capacitive manometer readings as simulated by the model and as measured in the equipment; (d) length of the frozen layer as calculated by the model for the inner and outer zones (the gray shaded area indicate the time window between the observed onset and offset).

the above parameters in all the parameter estimation activities presented in this study.

The values of the model parameters are reported in Table 4. Note that the value of the heat-transfer parameter a_1 for the outer zone is greater than twice the one related to the inner zone; additionally, the outer-zone mass-transfer parameter A is almost twice the one in the inner zone. This means that during sublimation, heat transfer and mass transfer are much stronger in the outer zone than in the inner one.

The estimates for C_2 are almost identical for the two zones, indicating that the contribution of the chamber pressure to the heat-transfer coefficient is roughly the same in the two zones. This is the reason why, for each of the subsequent case studies, we estimated only one value of C_2.

The values for a_3 in both zones are not reported in Table 4 because, during the estimation exercise, they always hit the assigned lower bound (1×10^{-8} [-]). This suggested that the contribution of radiation from the shelf surface to the vial bottom surface is almost negligible. Therefore, we decided not to consider this parameter in all the following experiment design activities and to set it to its lower bound. Finally, the values of the pressure correction parameters P_{bias} and γ resulted 0.18 Pa and 0.26 [-], respectively.

The prediction fidelity of the identified model for the base case is evaluated using the validation experiment reported in Figure 4. Note that in this figure and all subsequent ones illustrating experimental temperature profiles, the reported data are shown up to the registered inflection point. Also note that in this case we used as a validation experiment one that had been stopped before the primary drying phase was completed. Although the inner T_B is slightly underestimated with respect to the experimental evidence for a short time (Figure 4b; 2.5−5.5 h), the overall model performance in predicting the bulk temperature profile is good both in the inner zone and in the outer one, and this makes the model suitable for use in PT and CoV exercises.

3.2. Product Transfer. We used MBDoE to design an experiment to be carried out in EQUIP #2 in such a way as to re-estimate the model parameters for the new configuration. The parameter set considered in the design was A (inner and outer zone), a_1 (inner and outer zone), C_1, C_2, and α_{cd}.

When the product manufacturing is transferred to the new equipment, we expect that radiation effects (a_1) may be different from those encountered in EQUIP #1 (e.g., because of different distances between the shelves or to different surface emissivity). The equipment geometry may also impact the way other heat transfer-related parameters (C_1, C_2, α_{cd}) are affected by the chamber pressure. Finally, mass transfer (A), which depends on the resistance of the product cake, may be strongly related to how the equipment responds to the freezing step.[20,21]

To design the experiment for EQUIP #2 (step 1 in Section 2.1), we assumed that the initial estimates of the model parameters were the values pertaining to the base case. We also updated the values of the total number of vials, of the fraction of vials in the inner zone, and of the chamber volume (as indicated in Table 2 for EQUIP #2). It is worth noticing that the model used in the MBDoE task may require providing information about the new experimental setup that is not available a priori to the user. In the PT exercise, this occurred for the wall temperature in EQUIP #2. In the absence of this information, we carried out the experiment design assuming that the mean wall temperature was equal to the value that was measured for EQUIP #1 (276.15 K). After obtaining the optimal protocol for EQUIP #2, we run the designed experiment on EQUIP #2, then we determined the actual

https://dx.doi.org/10.1021/acs.iecr.0c03115
Ind. Eng. Chem. Res. 2020, 59, 20071−20085

Table 5. Parameter Estimates for the PT Exercise

	parameter [units]	estimate	std. deviation	*t*-value 95%
inner zone	A [s^{-1}]	2.35×10^{8}	4.66×10^{5}	257.2
	a_1 [m^2]	3.26×10^{-5}	1.40×10^{-7}	118.0
outer zone	A [s^{-1}]	2.63×10^{8}	1.47×10^{6}	91.3
	a_1 [m^2]	2.36×10^{-4}	7.18×10^{-7}	167.7
zone independent	C_1 [W m^{-2} K^{-1}]	2.95	4.56×10^{-2}	33.1
	C_2 [W m^{-2} K^{-1} Pa^{-1}]	0.83	5.64×10^{-3}	75.1
condenser	α_{cd} [s kg^{-1} K^{-1}]	8.18×10^{3}	19.52	213.7
		reference *t*-value 95%		1.645

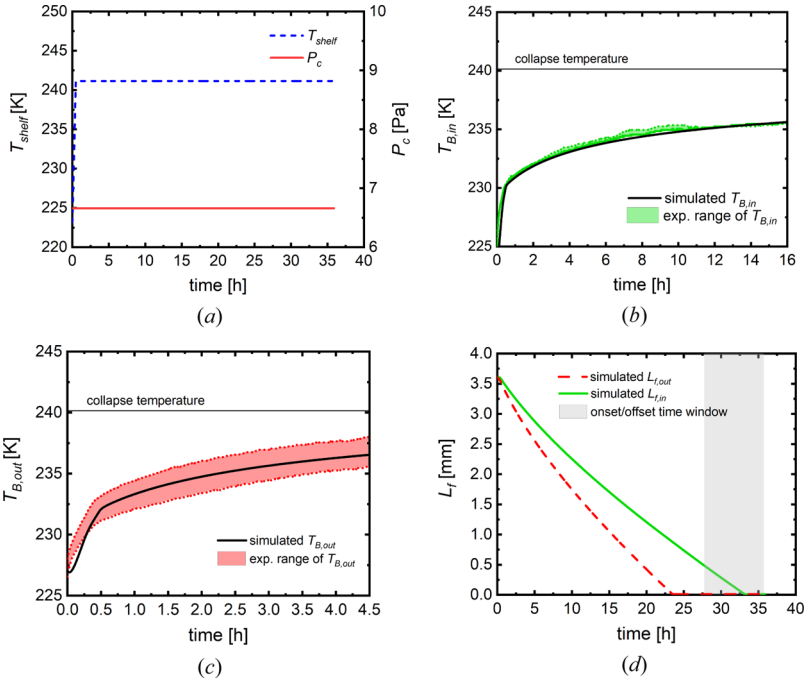

Figure 6. PT: model validation. Time profiles of (a) actual shelf temperature and chamber pressure; (b) bulk temperature in the inner zone as predicted by the model and as measured in the equipment; (c) bulk temperature in the outer zone as predicted by the model and as measured in the equipment; (d) length of the frozen layer as predicted by the model for the inner and outer zones (the gray shaded area indicate the time window between the observed onset and offset). The experimental temperature profiles in a zone are reported as the range between the maximum and minimum readings from the sensors in that zone.

mean wall temperature for EQUIP #2, and we finally proceeded with the model calibration/validation exercises using this actual value.

The resulting optimal experimental protocol is shown in Figure 5a. Inspection of the designed recipe shows that, at first, the shelf temperature is ramped up to 246 K at constant and low pressure (right above the assigned lower bound of 5 Pa). This combination of operating conditions clearly promotes greater sublimation rates. After this initial step (lasting about half an hour), the shelf temperature is increased up to ∼250 K at a lower rate, then it is gradually decreased, reaching the value of 225.15 K at ∼4.8 h from the beginning of the lyophilization cycle. In the meantime, the chamber pressure is assigned values in the range 6−9 Pa when the shelf temperature is still high (most probably to avoid violating the constraint on the maximum bulk temperature), and then it is decreased back to the initial value when the shelf temperature has already started to drop. In the remaining part of the experiment, the shelf temperature is kept practically constant, whereas the chamber pressure is gradually increased up to 12 Pa.

Following step 2 in Section 2.1, we carried out the designed experiment in EQUIP #2, and this allowed us to reidentify the model. Note that beyond the designed time interval (t > 10 h), the experiment was run at constant pressure (12 Pa) and shelf temperature (245.15 K) in order to complete the primary drying phase and obtain information about the end of sublimation. The new set of parameter estimates is summarized in Table 5. A remarkable result is that all parameter estimates were statistically satisfactory (*t*-values greater than the reference) after one single, optimally designed experiment (requiring no vial weighing). As observed in Section 2.1, had the estimate of any parameter been statistically unsatisfactory, one would have iterated the procedure using the updated parameter set to design a new experiment.

Focusing on the parameter estimates, we observe that the mass transfer-related parameter A for the outer zone is slightly greater (12%) than the one for the inner zone. If we compare this result with the base case (A for the outer zone was 83% greater than for the inner zone), we conclude that the experiment used for model calibration in EQUIP #2 determines a greater homogeneity in the cake structure between vials located at different positions in the shelf.

https://dx.doi.org/10.1021/acs.iecr.0c03115
Ind. Eng. Chem. Res. 2020, 59, 20071−20085

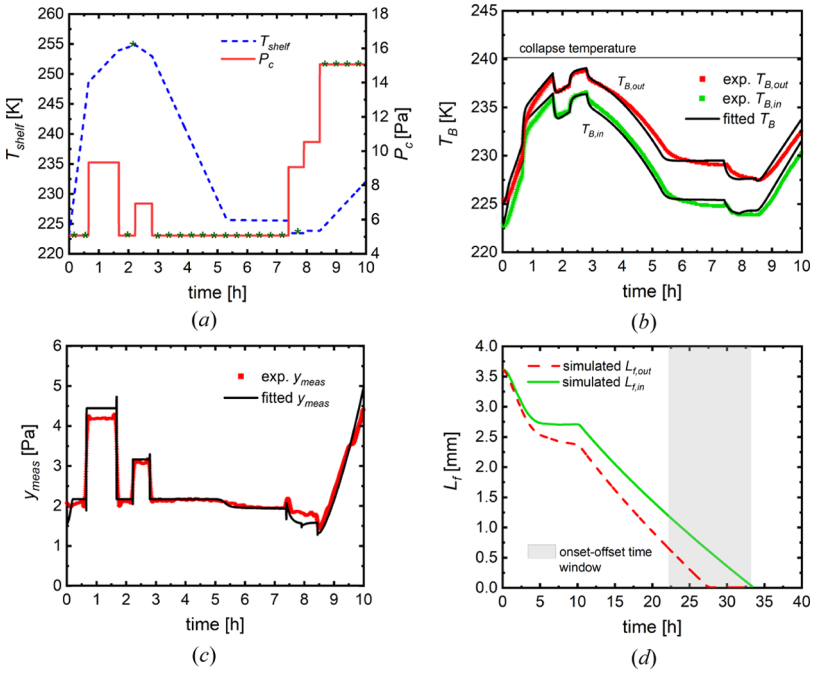

Figure 7. CoV: model calibration using an optimally designed experiment. Time profiles of (a) actual shelf temperature and chamber pressure as dictated by the optimally designed experiment (the green stars indicate pressure or temperature values that hit lower/upper bounds); (b) bulk temperature in the inner and outer zones as simulated by the model and as measured in the equipment; (c) difference between the Pirani and capacitive manometer readings as simulated by the model and as measured in the equipment; (d) length of the frozen layer as calculated by the model for the inner and outer zones (the gray shaded area indicate the time window between the observed onset and offset).

The values obtained for a_1 in the two different zones show that the contribution of thermal radiation for the outer zone is 6% greater than for the inner zone. Comparison with the base case (a_1 for the outer zone was 127% greater than for the inner zone value) leads to the conclusion that EQUIP #2 guarantees more homogeneity between vials than EQUIP #1. This statement is consistent with the fact that unlike EQUIP #2, (*i*) two frames are loaded for each shelf in EQUIP #1, and each frame is surrounded by a metallic rail and (*ii*) EQUIP #1 is equipped with a plexiglass window. Both factors contribute to increase thermal radiation in EQUIP #1, thus generating greater heterogeneity between vials closer to the window/rails and the rest of the charge in that equipment.

Parameter C_2 is about 3 times greater than the base case value, whereas C_1 is statistically invariant with respect to the base case. The latter result was expected, as C_1 describes the contribution because of heat transfer by conduction through the vial walls, which is not expected to change because the vials were not changed with respect to the base case. Variations in parameter C_2 as well as in α_{cd} seem to be (mostly) related to differences in equipment geometry and materials between different pieces of equipment (e.g., the shelves, as observed by Scutellà et al.[42]).

For the sake of completeness, the estimated values of the corrective parameters P_{bias} and γ were 2.58 Pa and 0.13 [-], respectively.

Figure 5 helps us to assess the model goodness-of-fit. The bulk temperature trajectories (Figure 5b) are captured very satisfactorily for both zones, and the actual bulk temperature never exceeds the collapse temperature. The difference between the Pirani and capacitive manometer readings (Figure 5c) is slightly underestimated when the chamber pressure and shelf temperature are both high, but the fit is good for the rest of the experiment. The frozen layer is calculated to vanish for the inner vials very close to the observed offset (Figure 5d).

Step 3 of the proposed methodology (Section 2.1) calls for model validation through an additional experiment. The protocol we used in the validation experiment is shown in Figure 6a and was selected to match the conditions in a typical run of the freeze-dryer. The model predictions are compared to the experimental evidence in Figure 6b–d. It can be seen that the model performance in predicting the bulk temperature profiles is very good. Furthermore, the predicted value of the sublimation end-point (length of the frozen layer of the inner vials equal to zero) is close to the midpoint.

3.3. Change of Vials. We used MBDoE to design a new experiment (Step 1) that processes the same formulation in the same freeze-dryer as in the base case but using a different type of vials (siliconized VIALS #2). The purpose of this experiment is to allow the identification of the model parameters under the new configuration.

The parameter set considered in experiment design was the same as for the PT exercise, with the addition of parameter R_0 because of the impact of the physical characteristics of the vial type on the physical structure of the processed formulated product.[19] The choice to re-estimate a_1 is related to the possibility that the surface emissivity for VIALS #2 is different from that of VIALS #1. The heat transfer-related coefficients (C_1, C_2) may be affected by the vial geometry, especially in relation to the vial bottom shape[20] and siliconization. Mass transfer (A) is related to cake resistance, which may change because of the different surface properties of the vials.[43] As occurred for the PT exercise, we assumed that the initial estimates of the model parameters for the new configuration were the values pertaining to the base case. The total number of vials, the fraction of the inner vials in the chamber, and the chamber volume were the same as is in the base case.

https://dx.doi.org/10.1021/acs.iecr.0c03115
Ind. Eng. Chem. Res. 2020, 59, 20071−20085

Table 6. Parameter Estimates for the CoV Exercise

	parameter [units]	estimate	std. deviation	*t*-value 95%
Inner zone	A [s^{-1}]	2.69×10^{8}	4.38×10^{5}	313.5
	a_1 [m^2]	3.47×10^{-6}	5.08×10^{-9}	34.9
Outer zone	A [s^{-1}]	3.37×10^{8}	1.10×10^{6}	157.3
	a_1 [m^2]	4.61×10^{-5}	9.11×10^{-8}	258.4
Zone independent	C_1 [W m^{-2} K^{-1}]	3.69	2.90×10^{-2}	65.1
	C_2 [W m^{-2} K^{-1} Pa^{-1}]	0.59	3.89×10^{-3}	77.1
	R_0 [m s^{-1}]	3.29×10^{4}	1.59×10^{2}	105.0
Condenser	α_{cd} [s kg^{-1} K^{-1}]	4.48×10^{4}	1.62×10^{2}	141.4
		reference *t*-value 95%		1.645

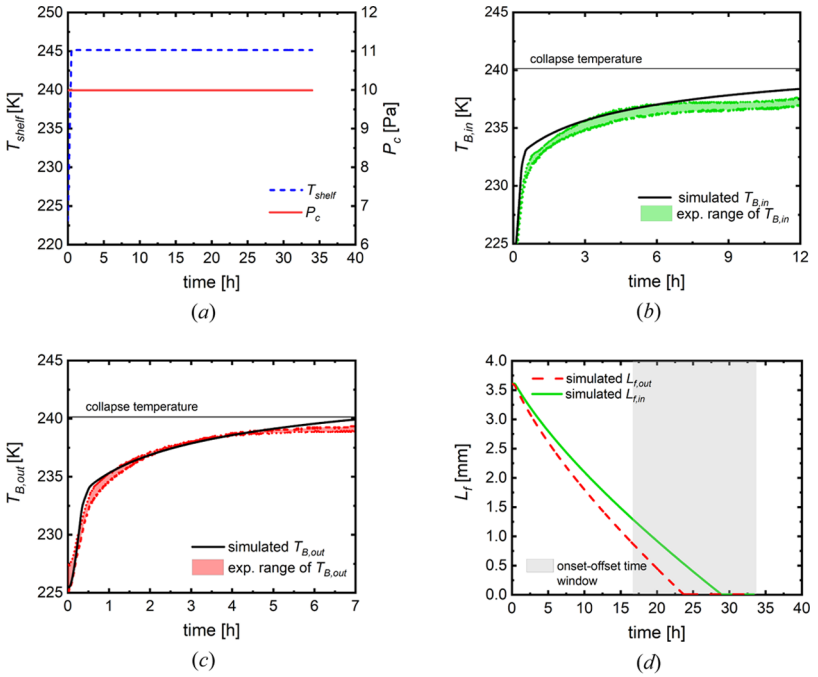

Figure 8. CoV: model validation. Time profiles of (a) actual shelf temperature and chamber pressure; (b) bulk temperature in the inner zone as predicted by the model and as measured in the equipment; (c) bulk temperature in the outer zone as predicted by the model and as measured in the equipment; (d) length of the frozen layer as predicted by the model for the inner and outer zones (the gray shaded area indicate the time window between the observed onset and offset). The experimental temperature profiles in a zone are reported as the range between the maximum and minimum readings from the sensors in that zone.

The resulting optimal protocol is shown in Figure 7a. The designed operating conditions are qualitatively similar to those obtained for the PT exercise, except for the shelf temperature peak (255 K), the maximum chamber pressure value at the end of the experiment (15 Pa), and the shelf temperature rise from 223.15 K (T_{shelf} lower bound) to 232 K in the final part of the protocol. After carrying out the experiment under the new configuration, we re-estimated the model parameters (Step 2), obtaining the results shown in Table 6. As in the PT exercise, all parameters were estimated precisely after one single experiment. As done for the PT exercise, the experiment was run at constant pressure (10 Pa) and shelf temperature (245.15 K) beyond the designed time interval (t > 10 h) in order to complete the primary drying phase and get the additional information about the end of sublimation.

We observe that the mass-transfer parameter A is greater (+25%) in the outer zone than in the inner one. Comparing this result with the base case (A for the outer zone was 83% greater than for the inner zone), we conclude that the mass-transfer resistance offered by VIAL #2 is more homogeneous than the one obtained with VIAL #1. The estimated values of a_1 for the inner and outer zones are much smaller than that in the base case (7 and 5% of the relevant base case values, respectively). This might be because of a significant difference in thermal radiation between the two vial types (i.e., VIAL #2 have probably lower emissivity than VIAL #1). The C_1 estimate is greater than both the base case value and the PT one, meaning that the conductive heat-transfer through the vial walls is greater for VIAL #2 than for VIAL #1. Changes in parameters C_2 and α_{cd} are likely to be related to the different interaction between vials and equipment geometry, particularly between the shelf and the bottom of the vial.

For the sake of completeness, the estimated values for the pressure correction parameters P_{bias} and γ were 1.33 Pa and 0.11 [-], respectively.

The fitting ability of the model under CoV can be appreciated in Figure 7b–d. The bulk temperature profiles are captured very well in both zones (Figure 7b). The difference between the Pirani and capacitive manometer readings (y_{meas}) is slightly overestimated at high chamber pressure and high shelf temperature conditions (Figure 7c), but overall the fitting is good. Finally, the frozen layer length

https://dx.doi.org/10.1021/acs.iecr.0c03115
Ind. Eng. Chem. Res. 2020, 59, 20071−20085

for vials in the inner zone is calculated to reach the value of zero at the observed offset time (Figure 7d). We also note that the actual bulk temperature never exceeds the collapse temperature. Overall, the model goodness-of-fit is very satisfactory.

Following step 3 of the proposed methodology, we performed a validation experiment under the same configuration. The operating recipe is shown in Figure 8a (P_c and T_{shelf} were kept constant as in typical freeze-drying runs), whereas Figure 8b−d compares the model predictions to the actual plant response. The temperature predictions (Figures 8b,c) are generally satisfactory, although a minor temperature overestimation occurs for both zones after ∼6 h from the start of the experiment. The time at which the sublimation is predicted to occur for the inner vials is close to the observed offset (Figure 8d; note that the time interval between the onset and the offset is very wide for this experiment). Overall, the performance of the model identified under the CoV configuration is very satisfactory.

4. CONCLUSIONS

In this study, we proposed to use MBDoEs to accelerate the development of pharmaceutical freeze-drying operations, with main emphasis on model calibration in the case of (i) PT/scale-up across different pieces of equipment and (ii) CoV. The main results obtained from this study can be summarized as follows:

1) A properly calibrated two-zone model of the lyophilization process can describe the time evolution of the process satisfactorily. Although this is a simplified model with some shortcomings (e.g., the dynamic evolution of the initial operation is not described accurately and sometimes temperature profiles are overestimated), it allows one both to represent the behavior of the majority of vials inside the drying chamber and to include at the experiment design level constraints on the maximum acceptable temperature for the product and on the maximum load to the condenser. This is a noteworthy difference from other commonly used experimental protocols for freeze-drying model parameter estimation.
2) One single, optimally designed experiment can be sufficient to obtain statistically meaningful estimates of all the key parameters related to heat and mass transfer.
3) The experimental burden required for model identification with the proposed framework is significantly smaller than using conventional approaches, such as those based on at least three gravimetric experiments and one complete primary drying experiment. The burden required by standard gravimetric experiments has been discussed elsewhere.[44] Based on the authors' industrial experience, three gravimetric experiments performed on a full-scale freeze-dryer (over 100,000 vial capacity) require approximately 3 weeks of occupancy of the equipment (and related labor), plus the manual weighing of a large number of vials. The procedure proposed in this study requires less than 1 day and no vial weighing at all.
4) Although, for the application considered in this study, MBDoE could in principle suffer from the initial parametric mismatch (e.g., the unknown heat- and mass-transfer parameters may change a lot with the equipment or vial type; the mean temperature of the condenser or of the vial walls or of the internal rails are not known a priori), it nevertheless proved very effective in terms of information gained by carrying out the optimally designed experiment.
5) Implementing Pirani and capacitive pressure readings as measured variables during the MBDoE stage is fundamental to compensate for the fact that the vial bottom temperature readings are in practice valid only until the temperature profiles inflect. Moreover, exploiting pressure measurements to detect the sublimation end-point events (onset, midpoint, offset) reduces the probability of getting stuck in local minima during the parameter estimation step. This makes the methodology particularly attractive also in production environments, where the availability of thermocouples/bulk temperature sensors may be limited.

In principle, the approach we have proposed to handle PT or vial change exercises can be easily extended to address also changes of the formulated product, an issue that is emerging as critical for the fast development of new vaccines or biopharmaceutical drugs.

Finally, we would like to point out that the proposed two-zone model is meant to allow practitioners to obtain, in a reasonably short amount of time, experimental protocols that can improve process understanding and characterization under configurations that are different from a given "base case" one. The concentrated parameter modeling assumption used in this study is however only a simplified description of the actual phenomena occurring inside a freeze-drying chamber, where the behavior of each single vial may differ from the one of any other vials in the chamber.[10] A further step in process optimization would therefore be to transfer the information obtained from the parametric estimates of the multizone model to a more representative multivial model.

AUTHOR INFORMATION

Corresponding Author

Massimiliano Barolo − *CAPE-Lab—Computer-Aided Process Engineering Laboratory, Department of Industrial Engineering, University of Padova, Padova 35131, Italy;* orcid.org/0000-0002-8125-5704; Email: max.barolo@unipd.it

Authors

Riccardo De-Luca − *CAPE-Lab—Computer-Aided Process Engineering Laboratory, Department of Industrial Engineering, University of Padova, Padova 35131, Italy*

Gabriele Bano − *GSK, Ware SG12 0DJ, U.K.*

Emanuele Tomba − *GSK, Siena 53100, Italy*

Fabrizio Bezzo − *CAPE-Lab—Computer-Aided Process Engineering Laboratory, Department of Industrial Engineering, University of Padova, Padova 35131, Italy;* orcid.org/0000-0003-1561-0584

Complete contact information is available at: https://pubs.acs.org/10.1021/acs.iecr.0c03115

Author Contributions

E.T. carried out the experiments and generated the experimental data. R.D.-L. and G.B. developed and coded the mathematical model, implemented MBDoEs, and analyzed the experimental results. All authors were involved in the result interpretation. R.D.-L. prepared the manuscript draft with important intellectual input from G.B., E.T., F.B., and M.B. All

https://dx.doi.org/10.1021/acs.iecr.0c03115
Ind. Eng. Chem. Res. 2020, 59, 20071−20085

authors were involved in revising the manuscript critically for important intellectual content. All authors had full access to the data and approved the manuscript before it was submitted by the corresponding author. The research was coordinated by M.B.

Notes

The authors declare no competing financial interest.

■ ACKNOWLEDGMENTS

This study was conducted under a cooperative research and development agreement between the University of Padova and GlaxoSmithKline Biologicals SA. GSK cosponsored this study in the framework of the University of Padova project "Uni-Impresa 2017—DIGI-LIO—toward digitalization of the pharmaceutical industry: generation of data with high information content for industrial freeze-drying process optimization".

■ NOMENCLATURE

General symbols

a_1, a_2, a_3	radiation heat-transfer parameters
$A_{b,v}$	vial bottom cross-sectional area
C_1, C_2, C_3	heat-transfer parameters
$c_{p,f}$	specific heat capacity of the frozen layer
d_v	vial diameter
$f(\cdot)$	differential and algebraic system implicit function
$f_{v,i}$	fraction of vials allocated to the ith zone
$\mathbf{G}(\cdot)$	set of active constraints
$h(\cdot)$	measurements selection function
J_w	sublimation flux
K_{cond}	heat-transfer coefficient due to conduction
K_{rad}	heat-transfer coefficient due to radiation from the shelves
L_0	length of the frozen layer at the beginning of primary drying
L_f	length of the frozen layer
$\dot{m}_{cd}$	water mass flow processed to the condenser
$\dot{m}_s^{tot}$	total sublimation mass flow
M_w	molecular weight of water
n_φ	number of design variables
N_{sp}	number of samples
N_V	number of vials
N_y	number of measured variables
N_{zones}	number of zones of the chamber
N_θ	number of model parameters
P_{bias}	corrective parameter
P_{cal}	pressure of Pirani gauge calibration
P_c	chamber pressure
P^{CM}	capacitance manometer pressure reading
$P_{w,c}$	water partial pressure in the chamber
$P_{w,c}^{exp}$	experimental value of water partial pressure
P^{Pir}	Pirani pressure reading
$P_{w,cd}$	partial pressure of water vapor at the condenser interface
$P_{w,int}$	water partial pressure at the sublimation interface
$Q_{r,v}$	radiation heat-transfer rate from the rails to the vial
$Q_{s,v}$	radiation heat-transfer rate from the shelf to the vial
$Q_{w,v}$	radiation heat-transfer rate from the chamber walls to the vial
R_0, A, B	mass-transfer parameters
R_g	ideal gas constant
R_P	resistance to mass transfer
s_{ij}	ijth element of the inverse matrix of measurement error
t	time
$t_{\theta_i}^{1-\alpha}$	t-value at $(1-\alpha)$ % confidence level for the ith parameter
$t_{ref}^{1-\alpha}$	reference t-value at $(1-\alpha)$ % confidence level
t^{sp}	vector of sampling times
$\overline{T}_{cd}$	mean temperature of the condenser surface
T_B	bulk temperature
$\overline{T}_r$	mean temperature of the rails
T_{shelf}	shelf temperature
$\overline{T}_W$	mean wall temperature
$\mathbf{u}(t)$	generic vector of manipulated variables
$\mathbf{V}_\theta$	variance-covariance matrix of model parameters
$\mathbf{V}_\theta^0$	initial value of variance-covariance matrix of model parameters
V_c	chamber volume
$\mathbf{w}$	vector of time-invariant control
$\mathbf{x}(t)$	vector of state variables
$\dot{\mathbf{x}}(t)$	vector of derivatives of state variables
y_{meas}	difference between Pirani and capacitive manometer readings
$\mathbf{y}_0$	vector of initial conditions
$\hat{\mathbf{y}}$	vector of estimated responses

Greek letters

α_{cd}	equipment-dependent parameter to describe $\dot{m}_{cd}$
γ	corrective coefficient
ΔH_{sub}	heat of sublimation
$\boldsymbol{\theta}$	vector of model parameters
v_{ii}	iith term of the parametric variance-covariance matrix
ρ_d	density of the dried layer
ρ_f	density of the frozen layer
σ_{SB}	Stefan−Boltzmann constant
τ	experimental duration
φ_i	ith component of the design vector
$\boldsymbol{\varphi}$	design vector
ψ	metric used for design optimization

Acronyms

CoV	change of vials
DAEBDF	differential-algebraic equation solver with backward differentiation formulae
MBDoE	model-based design of experiments
NLPSQP	nonlinear programming sequential quadratic approach
PT	product transfer

■ REFERENCES

(1) Nail, S. L.; Jiang, S.; Chongprasert, S.; Knopp, S. A. Fundamentals of Freeze-Drying. *Pharm. Biotechnol.* **2002**, *14*, 281−360.

(2) Chang, B. S.; Patro, S. Y. Freeze-drying Process Development for Protein Pharmaceuticals. *Lyophilization of Biopharmaceuticals*; American Association of Pharmaceutical Scientists: Arlington, VA, 2004; pp 113−138.

(3) Liu, Y.; Zhao, Y.; Feng, X. Exergy analysis for a freeze-drying process. *Appl. Therm. Eng.* **2008**, *28*, 675−690.

(4) Bjelošević, M.; Seljak, K. B.; Trstenjak, U. Aggressive conditions during primary drying as a contemporary approach to optimise freeze-drying cycles of biopharmaceuticals. *Eur. J. Pharm. Sci.* **2018**, *122*, 292−302.

(5) Rambhatla, S.; Obert, J. P.; Luthra, S.; Bhugra, C.; Pikal, M. J. Cake shrinkage during freeze drying: a combined experimental and theoretical study. *Pharm. Dev. Technol.* **2005**, *10*, 33−40.

https://dx.doi.org/10.1021/acs.iecr.0c03115
Ind. Eng. Chem. Res. 2020, 59, 20071−20085

(6) Depaz, R. A.; Pansare, S.; Patel, S. M. Freeze-drying above the glass transition temperature in amorphous protein formulations while maintaining product quality and improving process efficiency. *J. Pharm. Sci.* **2016**, *105*, 40−49.
(7) Patel, S. M.; Chaudhuri, S.; Pikal, M. J. Chocked flow and importance of Mach 1 in freeze-drying process design. *Chem. Eng. Sci.* **2010**, *65*, 5716−5727.
(8) Fissore, D.; Velardi, S. A.; Barresi, A. A. In-line control of a freeze-drying process in vial. *Dry. Technol.* **2008**, *26*, 685−694.
(9) Fissore, D.; Pisano, R.; Barresi, A. A. A model-based framework to optimize pharmaceuticals freeze-drying. *Dry. Technol.* **2012**, *30*, 946−958.
(10) Bano, G.; De-Luca, R.; Tomba, E.; Marcelli, A.; Bezzo, F.; Barolo, M. Primary drying optimization in pharmaceutical freeze-drying: a multi-vial stochastic modeling framework. *Ind. Eng. Chem. Res.* **2020**, *59*, 5056−5071.
(11) Sadikoglu, H.; Liapis, A. I. Mathematical modelling of the primary and secondary drying stages of bulk solution freeze-drying in trays: parameters estimation and model discrimination by comparison of theoretical results with experimental data. *Dry. Technol.* **1997**, *15*, 791−810.
(12) Velardi, S. A.; Barresi, A. A. Development of simplified models for the freeze-drying process and investigation of the optimal operating conditions. *Chem. Eng. Res. Des.* **2008**, *86*, 9−22.
(13) Sheehan, P.; Liapis, A. I. Modeling of the primary and secondary drying stages of the freeze drying of pharmaceutical products in vials: Numerical results obtained from the solution of a dynamic and spatially multi-dimensional lyophilization model for different operational policies. *Biotechnol. Bioeng.* **1998**, *60*, 712−728.
(14) Scutellà, B.; Trelea, I.-C.; Bourlés, E.; Fonseca, F.; Passot, S. Use of a multi-vial mathematical model to design freeze-drying cycles for pharmaceuticals at known risk of failure. *IDS. 21st International Drying Symposium Proceedings*; Editorial Universitat Politècnica de València, 2018; pp 315−322.
(15) Barresi, A. A.; Rasetto, V.; Marchisio, D. L. Use of Computational Fluid Dynamics for improving freeze-dryers design and understanding. Part 1: Modelling the lyophilisation chamber. *Eur. J. Pharm. Biopharm.* **2018**, *129*, 30−44.
(16) Fissore, D.; Pisano, R.; Barresi, A. A. Advanced approach to build the design space for the primary drying of a pharmaceutical freeze-drying process. *J. Pharm. Sci.* **2011**, *100*, 4922−4933.
(17) Pisano, R.; Fissore, D.; Barresi, A. A. Freeze-drying cycle optimization using model predictive control techniques. *Ind. Eng. Chem. Res.* **2011**, *50*, 7363−7379.
(18) Daraoui, N.; Dufour, P.; Hammouri, H.; Hottot, A. Model predictive control during the primary drying stage of lyophilization. *Contr. Eng. Pract.* **2010**, *18*, 483−494.
(19) Pikal, M. J.; Roy, M. L.; Shah, S. Mass and Heat Transfer in Vial Freeze-Drying of Pharmaceuticals: Role of the Vial. *J. Pharm. Sci.* **1984**, *73*, 1224−1237.
(20) Fissore, D.; Barresi, A. A. Scale-up and process transfer of freeze-drying recipes. *Dry. Technol.* **2011**, *29*, 1673−1684.
(21) Pisano, R.; Fissore, D.; Barresi, A. A.; Rastelli, M. Quality by design: scale-up of freeze-drying cycles in pharmaceutical industry. *AAPS PharmSciTech* **2013**, *14*, 1137−1149.
(22) Franceschini, G.; Macchietto, S. Model-based experimental analysis. *Chem. Eng. J.* **2008**, *63*, 4846−4872.
(23) Prasad, V.; Vlachos, D. G. Multiscale model and informatics-based optimal design of experiments: application to the catalytic decomposition of ammonia on ruthenium. *Ind. Eng. Chem. Res.* **2008**, *47*, 6555−6567.
(24) Galvanin, F.; Barolo, M.; Macchietto, S.; Bezzo, F. Optimal design of clinical tests for the identification of physiological models of Type 1 diabetes mellitus. *Ind. Eng. Chem. Res.* **2009**, *48*, 1989−2002.
(25) Chakrabarty, A.; Buzzard, G. T.; Rundell, A. E. Model-based design of experiments for cellular processes. *Wiley Interdiscip. Rev.: Syst. Biol. Med.* **2013**, *5*, 181−203.
(26) De-Luca, R.; Bano, G.; Tomba, E.; Bezzo, F.; Barolo, M. Model-based design of experiments to enable fast product transfer across freeze-drying units. *Proceedings of EuroDrying—7th European Drying Conference*; Euro Drying: Torino, Italy, 2019; pp 235−239.
(27) Abt, V.; Barz, T.; Cruz-Bournazou, M. N.; Herwig, C.; Kroll, P.; Möller, J.; Pörtner, R.; Schenkendorf, R. Model-based tools for optimal experiments in bioprocess engineering. *Curr. Opin. Chem. Eng.* **2018**, *22*, 244−252.
(28) Shahmohammadi, A.; McAuley, K. B. Sequential model-based A- and V-optimal design of experiments for building fundamental models of pharmaceutical production processes. *Comput. Chem. Eng.* **2019**, *129*, 106504.
(29) Asprey, S. P.; Macchietto, S. Statistical tools for optimal dynamic model building. *Comput. Chem. Eng.* **2000**, *24*, 1261−1267.
(30) Demichela, M.; Barresi, A. A.; Baldissone, G. The effect of human error on the temperature monitoring and control of freeze drying processes by means of thermocouples. *Front. Chem.* **2018**, *6*, 419.
(31) Patel, S. M.; Doen, T.; Pikal, M. J. Determination of end point of primary drying in freeze-drying process control. *AAPS PharmSciTech* **2010**, *11*, 73−84.
(32) Trelea, I. C.; Fonseca, F.; Passot, S.; Flick, D. A binary gas transport model improves the prediction of mass transfer in freeze drying. *Dry. Technol.* **2015**, *33*, 1849−1858.
(33) Pikal, M. J.; Bogner, R.; Mudhivarthi, V.; Sharma, P.; Sane, P. Freeze-drying process development and scale-up: scale-up of edge vial versus center vial heat transfer coefficients, Kv. *J. Pharm. Sci.* **2016**, *105*, 3333−3343.
(34) Pikal, M. J. Use of laboratory data in freeze drying process design: heat and mass transfer coefficients and the computer simulation of freeze drying. *A J. Pharm. Sci. Technol.* **1985**, *39*, 115−139.
(35) Fissore, D.; Pisano, R.; Barresi, A. A. Quality by design for Biopharmaceutical Drug Product Development. *AAPS Adv. Pharm. Sci. Ser.* **2015**, *18*, 565−593.
(36) Mortier, S. T. F. C.; Van Bockstal, P.-J.; Corver, J.; Nopens, I.; Gernaey, K. V.; De Beer, T. Uncertainty analysis as essential step in the establishment of the dynamic Design Space of primary drying during freeze-drying. *Eur. J. Pharm. Biopharm.* **2016**, *103*, 71−83.
(37) Scutellà, B.; Trelea, I. C.; Bourlès, E.; Fonseca, F.; Passot, S. Determination of the dried product resistance variability and its influence on the bulk temperature in pharmaceutical freeze-drying. *Eur. J. Pharm. Biopharm.* **2018**, *128*, 379−388.
(38) Pukelsheim, F. *Optimal Design of Experiments*; J. Wiley & Sons: New York, USA, 1993.
(39) Saltelli, A.; Chan, K.; Scott, E. *Sensitivity Analysis*; Wiley: Chichester, 2000.
(40) Zullo, L. *Computer Aided Design of Experiments. An Engineering Approach*; The University of London: London, UK, 1991.
(41) Vassiliadis, V. S.; Sargent, R. W. H.; Pantelides, C. C. Solution of class of multistage dynamic optimization problems. 1. Problems without path constraints. *Ind. Eng. Chem. Res.* **1994**, *33*, 2111−2122.
(42) Scutellà, B.; Passot, S.; Bourlés, E.; Fonseca, F.; Trelea, I. C. How vial geometry variability influences heat transfer and product temperature during freeze-drying. *J. Pharm. Sci.* **2017**, *106*, 770−778.
(43) Ditter, D.; Mahler, H.-C.; Roehl, H.; Wahl, M.; Huwyler, J.; Nieto, A.; Allmendinger, A. Characterization of surface properties of glass vials used as primary packaging material for parenterals. *Eur. J. Pharm. Biopharm.* **2018**, *125*, 58−67.
(44) Tang, X.; Nail, S. L.; Pikal, M. J. Freeze-drying process design by manometric temperature measurement: Design of a smart freeze-dryer. *Pharm. Res.* **2005**, *22*, 685−700.

https://dx.doi.org/10.1021/acs.iecr.0c03115
Ind. Eng. Chem. Res. 2020, 59, 20071−20085